URSI GASS 2020, Rome, Italy, 29 August - 5 September 2020

Self-Holography - Slimming Down Calibration of Large Aperture Arrays

C.R. Wilke[(1)], S.J. Wijnholds[(2)(1)], and J. Gilmore[(1)]
(1) Dept. Electrical and Electronic Engineering, Stellenbosch University, Stellenbosch, South Africa
(2) Netherlands Institute for Radio Astronomy (ASTRON), Dwingeloo, The Netherlands

Abstract

The Mid-Frequency Aperture Array (MFAA) of the Square Kilometre Array (SKA) operating in the 450-1450 MHz range is envisaged to have stations (subarrays) with $\sim 10^3$ to $\sim 10^4$ receive paths. Standard calibration procedures are based on the array covariance matrix which, at this scale, becomes extremely computationally expensive. Alternative, computationally cheaper approaches are in development and some have been proven to work. In this paper, we will focus on a method called self-holography, one of these approaches. Previous studies on self-holography showed that a bias in the gain estimates is caused by factors such as signal interference and system noise. In this paper, we investigate the effectiveness of reducing interference using null placement and subsequently reducing the bias on the gain estimates.

1 Introduction

Phased arrays have, for a long time, been a very attractive option for radio astronomy instruments. This is mainly due to their electronic steering capabilities, which is a very convenient alternative to mechanical steering. Additionally, they can form multiple beams on the sky [1][2]. This enables the exploration of interesting new science cases. The Mid-Frequency Aperture Array (MFAA), designed to operate in the 450 - 1450 MHz range, is an extreme example of this [3].

The MFAA is envisaged to have subarrays (or stations) that have $\sim 10^3$ to $\sim 10^4$ receive paths. Calibration of these subarrays is essential for achieving optimal beamforming performance. Traditional calibration schemes make use of the array covariance matrix, which implies that the computational complexity scales with the square of the number of receive paths [4][5]. Self-holography (SH) [6], which is based on the correlation of the individual receive paths against a signal from a reference beam formed by the full array, aims to reduce the processing load to scale linearly with the number of receive paths. The initial study in [6] found that a bias in the gain estimates are observed that is directly related to the signal to noise ratio (SNR) of the calibration measurements. In [7] it was concluded that this can only be remedied by careful modelling of the system noise. The closely related EPICal method [8] avoids this bias by using a full source model. This method effectively computes the full array covariance matrix during the data prediction stage needed for calibration, which comes with a computational cost.

In [9] a new rigorous approach is presented where it is assumed that the reference beam provides sufficient isolation of the calibration source. However, in reality, interfering sources will be present and it was determined that this causes a bias in the gain estimates. In this paper we investigate the effectiveness of mitigating that bias using null placement.

2 Self-holography

Assuming the narrowband condition holds, the output voltage x of an antenna receiving a signal s at time t can be expressed as

$$x(t) = g \cdot s(t) + n(t), \tag{1}$$

where g is the complex valued receive path gain, which is assumed to be constant over the calibration interval, and $n(t)$ is the noise in the receive path. If the antenna output voltage is exactly Nyquist sampled, the number of real valued samples produced for an integration time of τ seconds, will be equal to $N = 2 f_{max} \tau$. For an array of P receive paths, we can stack the measured samples for all receive paths in a vector $\mathbf{x}(t)$ and stack all these vectors in a $P \times N$ matrix $\mathbf{X} = [\mathbf{x}(0), \ldots \mathbf{x}((N-1)T)]^T$. Similarly, we can stack the samples of the signal and noise in matrices $\mathbf{S}$ and $\mathbf{N}$, so that we can describe the entire measurement by:

$$\mathbf{X} = \mathbf{G}\mathbf{S} + \mathbf{N}, \tag{2}$$

where $\mathbf{G}$ is a diagonal matrix with the gains of the receive paths placed on the main diagonal.

A reference beam signal $\mathbf{y}$ is obtained by multiplying the measured signals with the beamformer weights $\mathbf{w}$:

$$\mathbf{y} = \mathbf{w}^H \mathbf{X}, \tag{3}$$

where $\mathbf{w}$ is a $P \times 1$ vector containing the weights for each antenna, and $\mathbf{y}$ is the $1 \times N$ row vector containing the reference signal samples. The superscript ^{H} indicates the Hermitian transpose.

The expected value of the crosscorrelations between the reference signal and antenna signals $\mathbf{r}_{xy}$ is then calculated as:

$$\begin{aligned}\mathbf{r}_{xy} &= \varepsilon\{\mathbf{X}\mathbf{y}^H\} \\ &= \mathbf{G}\Sigma_s\mathbf{G}^H\mathbf{w} + \Sigma_n\mathbf{w},\end{aligned} \tag{4}$$

where Σ_s and Σ_n are the covariance matrices for the received and noise signals respectively. The noise covariance matrix is diagonal.

Next we calculate the expected value of the autocorrelations $\mathbf{r}_{xx}$ of the receive paths as:

$$\begin{aligned}\mathbf{r}_{xx} &= \text{vecdiag}\left(\varepsilon\{\mathbf{X}\mathbf{X}^H\}\right) \\ &= \text{vecdidag}\left(\mathbf{G}\Sigma_s\mathbf{G}^H\right) + \sigma_n,\end{aligned} \tag{5}$$

where vecdiag() converts the main diagonal of its argument into a vector.

At this stage we have $2P$ equations with $2P$ unknowns, namely $\mathbf{g} = \text{vecdiag}(\mathbf{G})$ and $\sigma_n = \text{vecdiag}(\Sigma_n)$. Next we express the problem as a matrix equation:

$$\begin{bmatrix}\mathbf{r}_{xy} \\ \mathbf{r}_{xx}\end{bmatrix} = \begin{bmatrix}\text{diag}\left(\Sigma_s\mathbf{G}^H\mathbf{w}\right) & \text{diag}\left(\mathbf{w}\right) \\ \text{diag}\left(\text{vecdiag}\left(\Sigma_s\mathbf{G}\right)\right) & \mathbf{I}\end{bmatrix}\begin{bmatrix}\mathbf{g} \\ \sigma_n\end{bmatrix}, \tag{6}$$

where $\mathbf{I}$ is the identity matrix. We can write the problem as:

$$\mathbf{r} = \mathbf{A}\mathbf{u}, \tag{7}$$

where $\mathbf{u}$ contains the unknown gains and noise powers, as indicated above, and can be solved as:

$$\mathbf{u} = \mathbf{A}^{-1}\mathbf{r}. \tag{8}$$

When solving, it is assumed that a calibration source is located in the phase centre and that there are no interfering signals present. As a result, all entries of Σ_s will be equal to the power of the calibration source which removes the need to model P^2 unique entries.

3 Simulation model

A 24-by-24 element uniform rectangular array (URA) with half-wavelength spacing is considered. A calibration source is located in the main beam of the array while an interfering source is located at a certain angle away from the main beam. Since we want to determine the effectiveness of nulling specifically, we are assuming a measurement scenario with zero system noise power. Measurements are generated and then multiplied with the true gains which are modelled as $g_p = CN(1, 0.1)$, i.e., gains nominally equal to unity with Gaussian noise on the real and imaginary component with a standard deviation of 0.1.

Two simulation scenarios are investigated:

1. The boresight angle of the interferer is varied between 10 and 85 degrees while the power of the interferer is constant and equal to the power of the calibration source.
2. The boresight angle of the interferer matches the first sidelobe of the array and its power is varied.

In both cases, a null is placed at the location of the interferer. The null is applied by multiplying the antenna signals with the appropriate weights that are calculated as:

$$\mathbf{w}_{\text{null}} = \mathbf{a}_c - \mathbf{a}_i\frac{\mathbf{a}_i^H\mathbf{a}_c}{\mathbf{a}_i^H\mathbf{a}_i}, \tag{9}$$

where $\mathbf{a}_c$ and $\mathbf{a}_i$ are $P \times 1$ vectors containing the geometric delay phasors of the antennas towards the calibration and interfering source respectively. This changes (3) to $\mathbf{y} = \mathbf{w}_{\text{null}}^H\mathbf{X}$.

4 Results

Scenario 1: interferer with variable position

Figure 1 shows a comparison of the mean magnitude and phase error of the gain estimates as a function of interferer boresight angle with nulling enabled and disabled.

When nulling is disabled, it is seen that the mean error follows the sidelobe pattern of the array. This is expected since, as explained earlier, the estimation error is directly proportional to the level of interference. Without nulling, the level of interference is mainly influenced by the sidelobe pattern of the array, which is a combination of the array factor and the average embedded element pattern (EEP).

With nulling enabled, it is seen that the mean error decreases as the interferer boresight angle increases. However, the level of error is similar to the level achieved in the nulls of the sidelobe pattern. This is an intuitive result as, at those locations, the inferfering source is nulled even without nulling that direction specifically. The error curve also indicates that the errors are non-zero. This is caused by the fact that the total power detected on the autocorrelations of the element signals is still the sum of the power of the two sources as detected by the individual elements in the array. As our simulations are based on a finite-length time series based on noise-like signals, this causes a self-noise effect [10]. As the power picked up from the interfering source is directly proportional to the embedded element patterns (EEPs) of the array, the mean error level gradually decreases to zero as the boresight angle increases.

Scenario 2: interferer with variable power

Figure 2 shows a comparison of the mean magnitude and phase error of the gain estimates as a function of Signal-to-Interference Ratio (SIR). The SIR is calculated as $\text{SIR} = P_c/P_i$, where P_c and P_i are the incident power, which is close to the apparent power as the EEPs hardly attenuate the signal at the small boresight angle used.

When comparing the results, it is evident that the null is highly effective in minimising the estimation error for the full range of interferer powers being considered. When nulling is disabled, we see a steady increase in estimation error followed by a discontinuity. Analysis of the gain solutions showed that this is the point where the calibration procedure switches to the interferer because of its dominant power.

When the power of the interferer is increased further, calibration with nulling enabled also breaks down. A detailed analysis in which we varied the length of the time series used as well as the magnitude of the gain errors in the array indicated that this is due to a combination of self-noise and beam errors at the start of the calibration iterations. The beam errors limit the suppression of the interferer while the self-noise restricts the achievable calibration accuracy in the first iteration of the calibration loop. As consecutive iterations are based on exactly the same time series, i.e., no new measurement is simulated, the iterations lock-in to an erroneous solution. Figure 3 shows a comparison of the phase estimation error of all antennas per iteration for SIR values of 0 dB and -20 dB. Notice the difference in convergence in the first few iterations between the two scenarios.

5 Conclusion

This paper explored null placement as a way of improving the performance of calibration using self-holography. Two dynamic simulation scenarios were used to summarise the possible improvements. The results from the first scenario showed that, while null placement is highly effective in reducing the error, there is still a dependence on the embedded element patterns. This was expected since it was previously determined that with interferers present, the self-holography method produces a bias that is dependent on both the array pattern and the embedded element pattern. The results from the second scenario showed that null placement remains highly effective even when the interfering power increases significantly.

These analyses were done for a 24-by-24 element URA. The performance of self-holography is strongly dependent on array size, so it is expected that these results will improve for larger arrays, such as the MFAA, which this work is aimed at. Both scenarios considered only one interferer, which is slightly unrealistic in a practical sense. The MFAA will be built in a radio-quiet environment, so it is expected that interference will be minimal. However, if momentarily significant interference does arise, it is likely that it will come from a single source. RFI monitoring stations should be able to detect it and its location. Nulling can then be used to minimise its impact. Nulling can also be used to suppress the signals from other bright astronomical sources that may have a detrimental effect on a calibration measurement on a pre-selected astronomical calibration source.

6 Acknowledgements

This work is supported by the National Research Foundation (NRF) of South Africa, the South African Radio Astronomy Observatory (SARAO) and by the Netherlands Organisation for Scientific Research.

References

[1] C. A. Balanis, *Antenna Theory*, 2nd ed. John Wiley & Sons, 1997.

[2] R. J. Mailloux, *Phased Array Antenna Handbook*, 3rd ed. Artech House, 2018.

[3] W. A. van Cappellen *et al.*, "MANTIS: The Mid-Frequency Aperture Array Transient and Intensity-Mapping System," https://arxiv.org/abs/1612.07917, Dec. 2016, MANTIS white paper.

[4] K. F. Warnick, R. Maaskant, M. V. Ivashina, D. B. Davidson, and B. D. Jeffs, *Phased Arrays for Radio Astronomy, Remote Sensing, and Satellite Communications*. Cambridge University Press, 2018.

[5] S. J. Wijnholds, S. van der Tol, R. Nijboer, and A.-J. van der Veen, "Calibration challenges for future radio telescopes," *IEEE Signal Processing Magazine*, vol. 27, no. 1, pp. 30–42, jan 2010. [Online]. Available: http://ieeexplore.ieee.org/document/5355494/

[6] S. J. Wijnholds, "Calibration of Mid-Frequency aperture array stations using self-holography," in *2017 International Conference on Electromagnetics in Advanced Applications (ICEAA)*, Sep. 2017, pp. 967–970.

[7] C. R. Wilke, S. J. Wijnholds, and J. Gilmore, "Performance Improvement of Self-Holography Based Aperture Array Station Calibration," in *European Conference on Antennas and Propagation (EUCAP)*, Krakow (Poland), 31 Mar. - 5 Apr. 2019.

[8] A. P. Beardsley, N. Thyagarajan, J. D. Bowman, and M. F. Morales, "An efficient feedback calibration algorithm for direct imaging radio telescopes," *Monthly Notices of the Royal Astronomical Society*, vol. 470, no. 4, pp. 4720–4731, Oct. 2017.

[9] C. R. Wilke, S. J. Wijnholds, and J. Gilmore, "Calibration of Large Aperture Arrays using Self-Holography," in preparation.

[10] S. Kulkarni, "Self-Noise in Interferometers: Radio and Infrared," *Astronomical Journal*, vol. 98, no. 3, pp. 1112–1130, Sep. 1989.

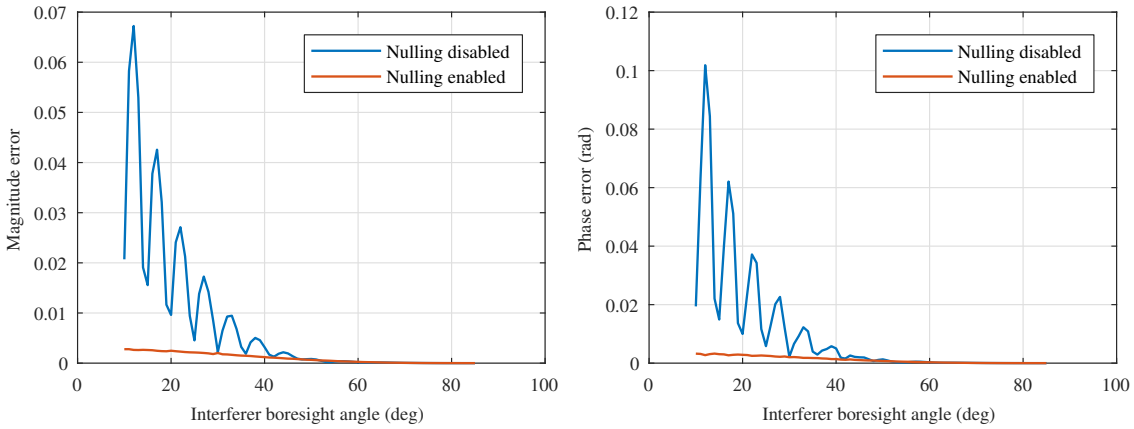

Figure 1. Error in magnitude (left) and phase (right) as a function of interferer boresight angle.

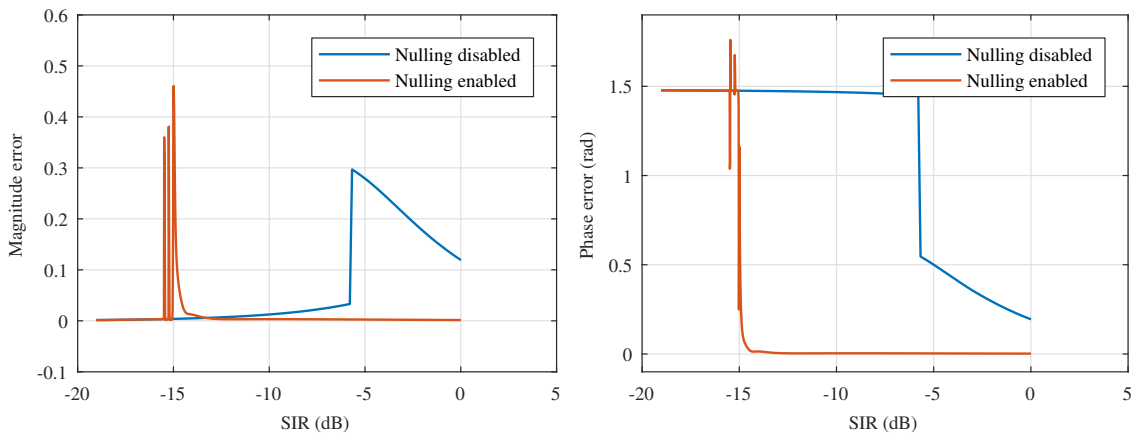

Figure 2. Error in magnitude (left) and phase (right) as a function of SIR.

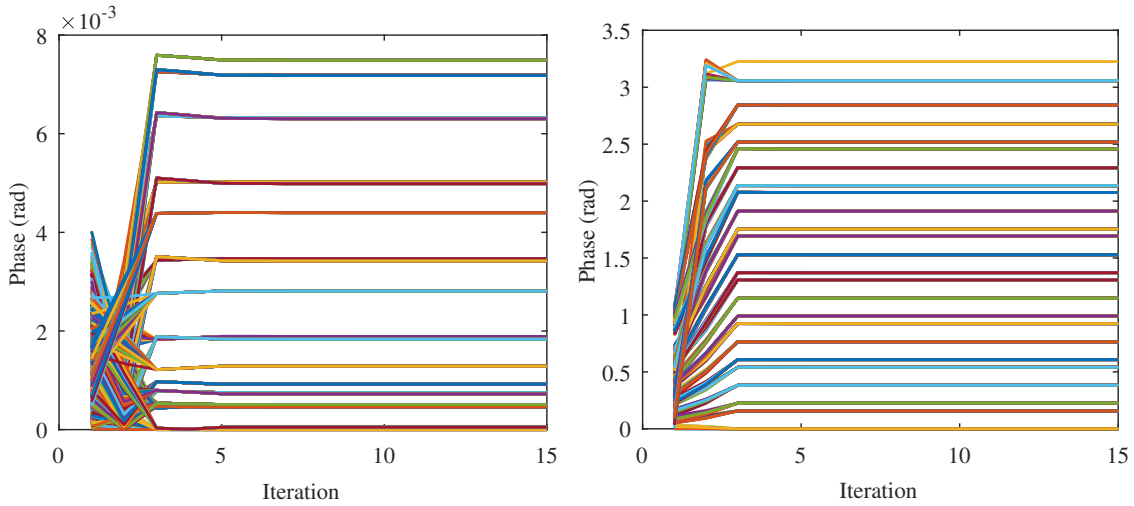

Figure 3. Phase estimate error of all antennas per iteration for SIR values of 0 dB (left) and -20 dB (right).